

Efficient Stein Variational Inference for Reliable Distribution-lossless Network Pruning

Yingchun WANG

The Hong Kong Polytechnic University
Hong Kong, China

20116342r@connect.polyu.hk

Weizhan Zhang
Xi'an Jiaotong University
Shan Xi, China

Jingcai Guo
The Hong Kong Polytechnic University
Hong Kong, China

Song Guo

The Hong Kong Polytechnic University
Hong Kong, China

song.guo@polyu.edu.hk

Yida Xu
Hong Kong Baptist University
Hong Kong, China

Jie Zhang
The Hong Kong Polytechnic University
Hong Kong, China

December 8, 2022

Abstract

Network pruning is a promising way to generate light but accurate models and enable their deployment on resource-limited edge devices. However, the current state-of-the-art assumes that the effective sub-network and the other superfluous parameters in the given network share the same distribution, where pruning inevitably involves a distribution truncation operation. They usually eliminate values near zero. While simple, it may not be the most appropriate method, as effective models may naturally have many small values associated with them. Removing near-zero values already embedded in model space may significantly reduce model accuracy. Another line of work has proposed to assign discrete prior over all possible sub-structures that still rely on human-crafted prior hypotheses. Worse still, existing methods use regularized point estimates, namely *Hard Pruning*, that can not provide error estimations and fail reliability justification for the pruned networks. In this paper, we propose a

novel distribution-lossless pruning method, named DLLP, to theoretically find the pruned lottery within Bayesian treatment. Specifically, DLLP remodels the vanilla networks as discrete priors for the latent pruned model and the other redundancy. More importantly, DLLP uses Stein Variational Inference to approach the latent prior and effectively bypasses calculating KL divergence with unknown distribution. Extensive experiments based on small Cifar-10 and large-scaled ImageNet demonstrate that our method can obtain sparser networks with great generalization performance while providing quantified reliability for the pruned model.

1 Introduction

Convolutional neural networks (CNNs) have achieved great success in many visual recognition tasks such as image classification [9], object detection [30], and image segmentation [3], etc. The success of CNNs is insepara-

ble from an excessive number of parameters that are well organized to perform sophisticated computations, which conflicts with the increasing demand for deploying these resource-consuming applications on resource-limited devices.

Network pruning has been an effective method to compress very deep neural networks without significant accuracy degradation. Guided by various heuristic regularizations, existing works identify a small enough sub-network with a deterministic point estimate that mimics the original performance. One of the most classic pruning methods is post-training pruning following an iterative three-stage paradigm: “training, pruning, and fine-tuning”, which is expensive and cumbersome. Recently, initialization pruning has been proposed as a promising method to identify an effective sub-network before training based on representative gradients, greatly reducing the computational overhead of iterative training [4, 31, 35]. Note that in the following we sometimes refer to lottery tickets to refer to the pruned submodel to be solved.

However, both post-pruning and initialization pruning are distribution-transacted, which leads to a great accuracy drop and unavoidably brings an extra fine-tuning cost. The fact lies in that existing methods model the inherently discrete lottery and model redundancies into one prior with a continuous distribution, which implicitly makes the deletion of sub-modules affect each other. Worse still, most of these works rely on heuristic parametric hypotheses to tackle the pruning optimization towards unknown prior. These subjective prior beliefs are lacking theoretical support, which may generate misleading and unreliable results, being difficult to convince the latent users. Last but not least, we have to say that state-of-the-art works are overconfident about their pruned results. Hard pruning with point estimate ignores the model estimation error from both aleatoric and epistemic uncertainties, leading to low estimator efficiency and resulting in poor pruning reliability.

In this work, we argue that *model pruning is a problem about the parameters distribution discovery with respect to the most causal sub-module for the latent variables*. We propose a novel distribution-lossless pruning method (DLLP) to perform more accurate model pruning. DLLP models the true low-dimensional prior as a spike-and-slab distribution and forces the learned model to approach the true prior by Stein variational inference.

Specifically, we explicitly assign two discrete distributions to the causal sub-module and redundant remainder. And different from previous methods using prior hyperparameters due to the unknown true distribution, DLLP bypasses directly solving the KL distance and uses the kernelized stein discrepancy between two distributions to calculate the gradient with respect to KL loss. So the approximate prior distribution parameterized by all learnable parameters can be optimized efficiently by stein variational gradient descent [21] with respect to KL distance loss together with experience risks. After that, the causal sub-module/pruned model would be the slap part of the optimized spike-and-slab distribution. Finally, as distribution-based estimation, DLLP can naturally provide the estimation error of both model’s prior and posterior, as well as the estimation efficiency. We theoretically demonstrate that DLLP significantly improves the estimation efficiency of the pruned model compared to the previous SOTA, thereby increasing the confidence of the results.

In summary, our contributions are:

- We theoretically analyze the pruning preliminaries from the most principled Bayesian perspective, and discover that the current pruning paradigm is distribution-truncated and relies on the heuristic hyperparameter hypothesis, inherently leading to significant accuracy reduction.
- We propose a novel distribution-lossless pruning method, named DLLP, to efficiently find the most accurate sub-model. The key lies in discrete prior modeling and deterministic stein variational inference.
- We subtly bypass computing the KL distance involving unknown distribution during pruning, and instead, we utilize the stein variational gradient to optimize along the steepest direction directly.

Extensive experiments on Cifar-10 and ImageNet datasets have demonstrated that DLLP achieves state-of-the-art pruning performance.

2 Related Work

2.1 Model Pruning

Most deep neural networks are overparameterized and unavoidably lead to expensive computing and memory over-

head [39]. Specifically, most deep networks have a large number of redundant parameters which contribute little to task performance. Previous works have demonstrated that only a small part (5-10%) of the weights are involved in the main calculation and lots of the activation values are zero. Thus, model pruning has been proposed to reduce the resource cost of deep models while keeping a satisfying accuracy.

Early works focus on pruning deep models based on the whole dataset and sharing a compact model among all different samples [18, 22, 27, 34, 37]. To be specific, static methods select pruning results through trade-offs on different samples, which leads to final compact models having limited representation capacity and thus suffering an obvious accuracy drop with large pruning rates.

Recently, some works turn their attention to the pursuit of the ultimate pruning rate and focus on excavating sample-wise model redundancy, named dynamic pruning. Dynamic pruning generates different compact models for different samples [5, 6, 14, 29, 32]. For example, [33] improves the dynamic pruning efficiency by embedding the manifold information of all samples into the space of pruned networks. Thus, dynamic methods could achieve a higher instance-wise compression rate. However, most dynamic pruning methods require deploying the full model and performing running time path-finding during inference. Thus, dynamic pruning is not resource-efficient and less practical.

2.2 Stein Variational Inference

Stein discrepancy is a measurement of the distance between probability distributions defined on a metric space, which is first formulated as a method to assess the quality of Markov chain Monte Carlo samplers. Based on that, [20] derives a statistical method to measure the difference between complex high-dimensional probability distributions, which combines the Stein feature and the reproduced kernel Hilbert space (RKHS), named Kernelized Stein Discrepancy (KSD). Unlike MCMC and VI, KSD has unbiased statistics which help to conduct hypothesis testing. The U-statistic of KSD depends only on the score function of the known distribution and does not depend on its normalization constant.

Taking KSD as the optimization target of the distribution, Liu Qiang et.al. [21] proposed an approximate

inference algorithm, Stein variational gradient descent (SVGD). Unlike Markov Chain Monte Carlo MCMC, it is a deterministic algorithm. SVGD is the natural counterpart to gradient descent applied in full Bayesian inference. Specifically, it performs (functional) gradient descent on this set of particles to minimize the KL divergence and drive the particles to fit the true posterior distribution. We take the optimization of SVGD in DLLP based on the following points: (1) The stein operator successfully makes the unknown distribution part of the distance calculation to 0, which eliminates the problem that the unknown distribution cannot be calculated; (2) The stein variation gives the analytical solution of the gradient direction with the fastest distribution change, which effectively increases the efficiency of optimization;

3 Method

In this section, we will provide a detailed illustration of the proposed **Distribution LossLess Pruning** (DLLP) method and the theoretical effectiveness guarantee. In Section 3.1, we first theoretically analyze previous pruning SOTAs from a principled Bayesian view, inherently revealing their essential deficiencies including distribution truncation and model unreliability. Then in Section 3.2, we discuss the two key technologies of DLLP with respect to prior distribution and stein variational inference. After that, we provide a theoretical guarantee of the model estimation efficiency of DLLP to demonstrate its effectiveness in Section 3.3.

3.1 Preliminaries

In this subsection, we analyze several existing model pruning works from a Bayesian perspective, including the classic pruning based on ℓ_1 , ℓ_2 regularization and weight magnitude and the cutting-edge polarization pruning based on batch normalization regularization.

3.1.1 Model Pruning From a Bayesian Perspective

Given a dataset with N samples as $X = \{x_i\}_{i=1}^N$ with the corresponding labels $Y = \{y_i\}_{i=1}^N$. We assume that the dataset follows a Gaussian distribution with variance δ and expectation y . For a convolution neural network

(CNN) with a parameter set Θ with M items, ω_i denotes the i_{th} learnable items in Θ . Assuming that the learnable model parameters follow a Laplace distribution prior with the expectation 0 and the variance b , we have $f(\Theta|0, b) = \frac{1}{2b} \exp^{-\frac{|\Theta|}{b}}$. Then, the posterior probability of the model under the current data conditions can be defined as:

$$p(\Theta|Y, X) \propto p(Y|X; \Theta)p(\Theta) \\ = \prod_{i=1}^N \prod_{j=1}^M \frac{1}{\sqrt{2\pi\delta}} \exp^{-\frac{(y_i - \omega_j x_i)^2}{2\delta}} \frac{1}{2b} \exp^{-\frac{|\omega_j|}{b}}, \quad (1)$$

and the log function of the conditional posterior of the referenced model is:

$$\log p(\Theta|Y, X) \propto - \sum_{i=1}^N \sum_{j=1}^M \left\{ \frac{1}{2\delta} (y_i - \omega_j x_i)^2 + \frac{1}{b} \|\omega_j\|_1 \right\} \quad (2)$$

Then we could get the familiar formulation of the ℓ_1 -norm regularization pruning [8]:

$$\Theta^* = \arg \min_{\Theta} \sum_{i=1}^N \sum_{j=1}^M \left\{ \frac{1}{2\delta} (y_i - \omega_j x_i)^2 + \frac{1}{b} \|\omega_j\|_1 \right\} \quad (3)$$

Similarly, assuming the model prior obeys Gaussian distribution with the expectation 0 and the variance α , the equivalent Bayesian form of ℓ_2 -norm regularization pruning can be derived as:

$$\Theta^* = \arg \min_{\Theta} \sum_{i=1}^N \sum_{j=1}^M \left\{ \frac{1}{2\delta} (y_i - \omega_j x_i)^2 + \frac{1}{2\alpha} \omega_j^2 \right\} \quad (4)$$

Another example comes from state-of-the-art neuron-level model pruning using polarization regularizer [40], where each neuron is associated with a scaling factor. Let γ represent the set of the scaling factors, and in Bayesian treatment, their γ follows the prior distribution as follows:

$$p(\gamma) = \frac{1}{2} \left(\frac{1}{2a} e^{-\frac{|\gamma - \bar{\gamma}|}{a}} - \frac{1}{2a} e^{-\frac{|\gamma|}{a}} \right), \quad (5)$$

where $\bar{\gamma}$ is the mean of all elements in γ and a denotes the variance of Laplace distributions. The model parameters are modeled as a Gaussian distribution with the hyperprior of γ as: $p(\Theta|\alpha, \gamma) = \frac{1}{\sqrt{2\pi\alpha}} e^{-\frac{(\gamma\Theta)^2}{2\alpha}}$. Thus, the opti-

mization of polarization neuron pruning is equal to minimizing the negative of the following posterior probability:

$$\log p(\Theta, \gamma|Y, X) \propto p(Y, X|\Theta, \gamma)P(\Theta|\gamma)p(\gamma) \\ \propto -\frac{1}{2\delta} \sum_{i=1}^N (y_i - \Theta x_i)^2 - \frac{(\gamma\Theta)^2}{2\alpha} + \frac{1}{a} (t\|\gamma\| - \|\gamma - \bar{\gamma}\|) \quad (6)$$

As shown in Eq. 3, Eq. 4, and Eq. 6, the optimization targets of existing SOTAs are equivalent to modeling the learnable parameters as Gaussian distributions with deterministic parametric hypotheses. However, such optimization would produce biased and inconsistent estimations for the pruned model due to the following two main limitations:

(1) **Prior sharing:** Instead of assigning discrete priors, existing SOTAs generalize all possible substructures into the same continuous prior, where pruning inevitably involves a distribution truncation operation. Liu et.al [24] have pointed out that the well-trained convolution models should approximately follow a Gaussian-like distribution. Therefore, distribution-truncated pruning could significantly reduce model accuracy. We will theoretically illustrate the distributional truncation from pruning in the next subsection.

(2) **Parametric hypothesis:** The current SOTAs heuristically set the hyperparameters in the unknown distribution as deterministic values instead of estimable random variables. While simple, it may generate misleading results and poor generalization performance. Worse still, we theoretically demonstrate that this artificial setting could significantly reduce the estimation efficiency of the pruned model. Estimators with low efficiency bring an unreliable pruned model, especially when facing uncontrollable data domains in the real world.

3.1.2 Distribution-truncated Pruning

In this subsection, we will analyze the distributions of the two parts of an overall Gaussian distribution which are torn apart by hard pruning, and explain the amount of information lost in distribution-loss pruning.

Let σ be the variance of model distribution in the unpruned model and n be the number of samples. Generally, the model parameters based on ℓ_1 -norm (Eq. 3) and ℓ_2 -norm (Eq. 4) regularization follow a **Half-normal distribution** and a **Scaled Chi distribution**, respectively. Define the power of norm terms as p (1 or 2), then the distribution of the model parameters obeys Amoroso($0, \sqrt{2}\sigma, \frac{n(p-1)}{2}, 2$) and can be written as follows:

$$p(\Theta) = \frac{1}{\Gamma(\frac{n(p-1)}{2})} \left| \frac{\sqrt{2}}{\sigma} \right| \left(\frac{\Theta}{\sqrt{2}\sigma} \right)^{n(p-1)-1} \exp\left(-\left(\frac{\Theta}{\sqrt{2}\sigma}\right)^2\right). \quad (7)$$

After training, hard pruning removes parts of estimators deemed unimportant under respective criteria. We use classical magnitude-based prune to illustrate this process. Assume Δ as the magnitude threshold. After removing ‘‘unimportant’’ weights smaller than Δ , the limit distribution of the reserved tail can be modeled as a generalized Pareto distribution (GPD) [28]. For a single item w_i in Θ , its probability density can be written as follows:

$$p(\omega_i) = \begin{cases} 0 & \text{if } |\omega_i| \leq \Delta \\ \frac{k\Delta^k}{\omega_i^{k+1}} & \text{else } |\omega_i| > \Delta \end{cases} \quad (8)$$

where $k = \frac{h}{\sigma}$, $h \in \mathbb{R}$ and $h > 0$. Removed nodes are part of the model prior distribution and contribute to model predictions.

3.2 Detailed DLLP

In this section, we will explain the implementation of DLLP from two aspects: (1) **discrete prior modeling** to overcome the biased and inconsistent estimation of the pruning model caused by the hypothetical and uniform model prior; (2) **stein variational inference** to take the estimator uncertainties of the pruned model into consideration instead of using point estimation. The detailed training pipeline of DLLP can be found in Algorithm. 1.

3.2.1 Prior Distribution

Given data likelihood:

$$p(Y|X, \Theta, d) = \frac{d}{\sqrt{2\pi}} e^{-\frac{d^2(Y-\Theta X)^2}{2}} \quad (9)$$

where d denotes the inverse of the variance of the predictions. Note that d is a learnable parameter in our method.

As discussed before, DLLP expects to automatically derive the most possible causal module by distribution-lossless model pruning. Thus, it assigns different priors to the pruned model and the remaining parts. Specifically, DLLP models the prior of the referenced networks as a spike-and-slab distribution which includes two discrete Gaussian distributions combined by a Bernoulli function. The details are expressed as follows:

$$p(\Theta|\lambda, \epsilon, \Phi) = \prod_{i=1}^M \left(\theta_i \frac{\lambda}{\sqrt{2\pi}} \exp\left(-\frac{(\lambda\omega_i)^2}{2}\right) + (1 - \theta_i) \frac{\epsilon}{\sqrt{2\pi}} \exp\left(-\frac{(\epsilon\omega_i)^2}{2}\right) \right) \quad (10)$$

where ϵ is a positive infinity and $\lim_{\epsilon \rightarrow \infty} \mathcal{N}(\omega_i|0, \frac{1}{\epsilon}) = \delta_0(\omega_i)$. $\lambda \in \mathbb{R}^+$ is a learnable parameter. θ_i is the probability for the Bernoulli distribution. For each variable ω_i , it belongs to the most possible causal sub-module with probability θ_i and obeys the gaussian distribution $\mathcal{N}(0, \frac{1}{\lambda})$. Instead, it follows $\mathcal{N}(0, \frac{1}{\epsilon})$ with probability $1 - \theta_i$. And Φ is the set of θ .

Then we could derive the weights posterior as follows:

$$p(\Theta|Y, X) \propto p(Y|X, \Theta, d) p(\Theta|\lambda, \epsilon, \Phi) = \prod_{i=1}^N \prod_{j=1}^M \mathcal{N}(\omega_j x_i, d) \left\{ \theta_j \mathcal{N}\left(0, \frac{1}{\lambda}\right) + (1 - \theta_j) \mathcal{N}\left(0, \frac{1}{\epsilon}\right) \right\} \quad (11)$$

In the following, we may abbreviate $p(\Theta|Y, X)$ as p_Θ . Assuming a variational distribution $q(\Theta)$ (q_Θ) to approximate the above posterior, the optimization of the model distribution during sparsity training can be constructed as follows:

$$q^*(\Theta) = \arg \min_q \max_p \text{KL} \{q(\Theta) || p(\Theta|Y, X)\} \quad (12)$$

3.2.2 Optimization Objective

DLLP is defined as a hybrid optimization with respect to the minimization of task loss and distribution distance. The overall objective is defined as:

$$\begin{aligned} \min \mathcal{J}(\Theta) &= \min \mathbb{E}_X \mathbb{E}_\Phi L_\Theta(X) \\ &= \min \mathbb{E}_X \mathbb{E}_\Phi [\mathcal{L}(f_\Theta(X), Y) + \beta \text{KL}(q(\Theta) || p(\Theta|Y, X))] \end{aligned} \quad (13)$$

where $f_\Theta(X)$ denotes the model predictions for input X , and β is a tuning hyperparameter to adjust the weights of the two optimization terms.

Note that the model prior is ambiguous with unknown normalization parameters, so it is hard to compute the accurate distance between $q(\Theta)$ and the target $p(\Theta|Y, X)$. Unlike previous work that uses heuristic assumptions to force the calculation of KL [1, 26], we cleverly bypass solving KL with unknown distributions and instead seek the optimal direction that makes the KL decrease the fastest. Specifically, we regard each model updating as a smooth transformation of $q(\Theta)$, and our goal is to find out an optimal transformation function corresponding to the maximum drop of the KL function. Define functional that maps all possible transformation directions of $q(\Theta)$ to the declines in the KL($q(\Theta)||p(\Theta|Y, X)$). It has been proved that the derivative direction of the functional is the negative of the kernelized stein discrepancy between the distributions [21], which can be described as:

$$\begin{aligned} & -S(q(\Theta)||p(\Theta|Y, X)) \\ & = -\mathbb{E}_{\Theta \sim q} [k(\Theta, \cdot) \nabla_{\Theta} \log p(\Theta|Y, X) + \nabla_{\Theta} k(\Theta, \cdot)] \end{aligned} \quad (14)$$

where k denotes a kernel function, which is a radial basis function kernel in DLLP.

To optimized the objective in Eq. 13, we can derive the gradients with respect to Θ as follows:

$$\begin{aligned} \nabla_{\Theta} \mathcal{J}(\times) & = \mathbb{E}_X \mathbb{E}_{\Phi} \nabla_{\Theta} L(\Theta, X) \\ & = \mathbb{E}_X \mathbb{E}_{\Phi} \nabla_{\Theta} \mathcal{L}(f_{\Theta}, Y) - \beta S(q(\Theta)||p(\Theta|Y, X)) \end{aligned} \quad (15)$$

The first part in Eq. 15 is the cross entropy loss of the task predictions while the other two parts correspond to the KL loss between the current model distribution and the target posterior. Note that we use the continuous Gumble-Softmax trick to sample possible weights from the discrete Bernoulli binomial distribution so that Eq. 13 can be optimized end-to-end in a gradient descent manner. And DLLP scales down the temperature of the gumble softmax during the training process to gradually approach the real discrete distribution.

Algorithm 1 Network pruning based on discrete prior modeling and efficient stein variational gradient descent.

Input:

A randomly initialized referenced model with learnable parameters set $M_0 = \{\Theta_0, d_0, \lambda_0, \{\theta_i\}^0\}$;
 Another twin model with $M_1 = \{\Theta_1, d_1, \lambda_1, \{\theta_i\}^1\}$;
 A target distribution $p(\Theta)$ as in Eq. 11.

Output:

The referenced model M_0 that approximates $p(\Theta)$;
 The pruned subpart M_p ;

```

1: repeat
2:    $K(\Theta_0, \Theta_1) = \exp(-\frac{1}{\log 2} \|\Theta_0 - \Theta_1\|_2^2) \leftarrow$  Compute the kernelized model distance;
3:    $(x_i, y_i) \leftarrow$  Randomly select a data batch;
4:   for  $m \in [M_0, M_1]$  do
5:      $\hat{y}_i \leftarrow$  Perform a model forward propagation ;
6:      $p(\Theta|y_i, x_i) \leftarrow$  Compute posterior probability based on Eq. 9, Eq. 10 and Eq. 11;
7:      $\Delta m \leftarrow$  Compute model gradient based on Eq. 14 and Eq. 15;
8:      $m \leftarrow$  Update model with gradient  $\Delta m$ 
9:   end for
10: until convergence of  $M_0$ 
11:  $M_p \leftarrow$  Extract the slab part from  $M_0$  which follows a spike-and-slab distribution;
12: return  $M_0, M_p$ 

```

3.3 Theoretical Guarantee

In this subsection, we will illustrate that the prior hypothesis and point estimation in the current SOTA severely reduces the estimation efficiency of pruned estimators, resulting in untrustworthy lightweight models. We first theoretically compute the ideal Cramer-Rao lower bound (CRLB) for the pruned estimators. Based on that, we provide the estimation efficiency of the current SOTA in four cases. The results show that existing pruning paradigms have poor credibility, thus being impractical in the noisy real world.

Given the set of data samples X , assume that the outputs of multiple forward passes obey the observation equation: $Y_k = \Theta \top X + n_k, k = 1, 2, \dots, N$, wherein K represents the number of observations, and n_k is an

independent and identically distributed Gaussian random noise with mean as 0 and variance as ϵ^2 . The estimator Θ is a Gaussian random variable with mean as μ_Θ and variance as α^2 , also, $\Theta \top X \sim \mathcal{N}(\mu_\Theta \top X, \alpha^2)$. Since X is a constant, in the following we would use Θ and $\Theta \top X$ interchangeably. Based on the optimization target defined in Eq. 11, Eq. 12 and Eq. 13, the maximum posterior estimator of Θ can be computed as:

$$\hat{\Theta}_{map} = \frac{\bar{Y}\alpha^2 + \mu_\Theta\epsilon^2}{\epsilon^2 + \alpha^2} \quad (16)$$

where $\bar{Y} = \frac{1}{K} \sum_{k=1}^K Y_k$. As in SOTAs which use the point estimator for pruned models, the variances of model parameters α^2 are confidently set to zero, and we have $\mathbb{E}[\hat{\Theta}_{map}] = \mathbb{E}[\Theta] = \mu_\Theta$. Under this condition, $\hat{\Theta}_{map}$ is an unbiased estimate of Θ , and $\mathbb{E}[\hat{\Theta}_{map} \top X - \Theta \top X] = \sum_{k=1}^\infty (Y_k - \Theta \top X) p(Y_k | X, \Theta) = 0$.

Thus, for a pruned model, the ideal CRLB of its unbiased estimator could be calculated as:

$$\mathbb{E}[\hat{\Theta}_{map} \top X - \Theta \top X] \geq \frac{1}{-\mathbb{E}\left[\frac{\partial^2 \ln p(Y_k | X, \Theta)}{\partial \Theta^2}\right]} \quad (17)$$

We note the lower bound of the pruned estimator as $\text{CRLB}(\hat{\Theta}) = \epsilon^2$.

Next, we discuss the estimation efficiency of the pruned model in four real-world cases, to illustrate the poor unreliability of pruning SOTAs.

X, Θ without noise: This ideal situation is the same as the setup in SOTA above. The estimator variance could be calculated as: $\text{Var}(\hat{\Theta}) = \text{Var}(Y_k) = \epsilon^2$, and the conditional estimation efficiency would be: $e(\Theta) = \frac{\text{CRLB}(\hat{\Theta})}{\text{var}(\hat{\Theta}_{map})} = 1$.

In fact, the point estimator of the pruned network is fully efficient if and only if neither the model training process nor the data distribution is noisy.

X without noise, Θ with noise: Assume there is a model uncertainty and $\alpha^2 \neq 0$. According to [16], $\text{Var}(\hat{\Theta}_{map}) \approx \epsilon^2 + \alpha^2$, and its estimation efficiency is: $e(\Theta) = \frac{\text{CRLB}(\hat{\Theta})}{\text{Var}(\hat{\Theta}_{map})} = \frac{\epsilon^2}{\epsilon^2 + \alpha^2} < 1$.

X with noise, Θ without noise: Similarly, assume $p(Y | X) \sim \mathcal{N}(0, \beta^2)$, the estimation efficiency would be: $e(\Theta) = \frac{\text{CRLB}(\hat{\Theta})}{\text{Var}(\hat{\Theta}_{map})} = \frac{\epsilon^2}{\epsilon^2 + \beta^2} < 1$.

X with noise, Θ with noise: With the same distribu-

tion assumptions, the estimation efficiency of the pruned model is: $e(\Theta) = \frac{\text{CRLB}(\hat{\Theta})}{\text{Var}(\hat{\Theta}_{map})} = \frac{\epsilon^2}{\epsilon^2 + \alpha^2 + \beta^2} < 1$.

It can be explicitly seen that as noise (data or model) increases, the validity of the pruned estimators could significantly decrease under the previous frame. The proposed DLLP can naturally improve the estimation efficiencies for both the pruned model and task prediction. At the same time, it also provides estimation errors, significantly increasing the reliability of the pruned networks. The relevant proofs of the formulas will be shown in the supplementary material.

4 Experiment

In this section, we perform extensive experiments to analyze and validate the effectiveness of the proposed DLLP. We first describe the experimental setup of DLLP in Section 4.1. Then, to study the effectiveness of the indirect KL distance optimization to both model distribution and task accuracy, we conduct ablation studies of the stein kernelized discrepancy based on the spike-and-slab distribution in Section 4.2. Finally, in Section 4.3, we compare the proposed DLLP with state-of-the-art model pruning methods with respect to both task performance and model reliability. More details and experiment results will be shown in Supplemental Materials.

4.1 Implement Details

4.1.1 Baseline

Model: We explore the effectiveness of our distribution-lossless pruning method on various popular network architectures. For VGG with plain architecture, we choose the widely-used VGG-16 BN with interspersed batch normalization layers. For ResNet with residual structure, we comprehensively select Bottleneck-style ResNet-50 and Basic-style ResNet-56. Despite the challenges, such extensive comparison more effectively confirms the broad applicability of the proposed DLLP.

Note that these networks are improved accordingly to DLLP. For example, we add a global variable for each network as a learnable parameter to capture the noise from the uncontrollable observation. Also, we add a learnable local variable for each convolution module

to model the insufficient model learning. Finally, each convolution parameter is associated with a Bernoulli variable to make a discrete choice about which of all possible sub-modules the parameter belongs to. To make the distribution sampling process differentiable, we use the continuous Gumble Softmax trick in practice.

Dataset: Some works have pointed out that the same pruning method may perform differently on datasets with different sample numbers. Thus, we use various popular image datasets in model pruning, including the small CIFAR-10 dataset and large-scaled ImageNet. Specifically, Cifar-10 contains only 60,000 nature color images uniformly distributed in 10 classes. While ImageNet, currently the largest database for image recognition, is more difficult to be predicted. It contains more than 1.2 million natural images and corresponds to 1000 categories.

4.1.2 DLLP Training

As discussed earlier, DLLP naturally induces the most causally pruned sub-modules in a one-shot training process by assigning different prior distributions to all possible sub-modules. The training process is conducted on 2 Nvidia GTX 3090TI GPUs. Each architecture is trained for 60 epochs to observe long-term effects. The batch size is set as 512 for all training. We start from the learning rate of 0.1 and gradually reduce it to 0.001. The only hyperparameter in our optimization objective is β which is empirically set as 0.1.

After optimization, we visualized the model distribution results under all architectures. Specifically, the pruned model derived by DLLP is a discrete sub-distribution from the original model distribution, while the pruned model obtained by all other methods is the sparse original model itself.

4.2 Ablation Study

4.2.1 Pruned Model Distribution

An important property of DLLP is that after pruning, DLLP should observe a smooth Gaussian distribution rather than a destroyed incomplete distribution. This phenomenon stems from the fact that the pruned model obtained by DLLP is an independent and most causal sub-

module in the original model, and there is no correlation between all possible sub-modules of the model. The pruned model obtained by other SOTA methods is the residual result after heuristically savagely deleting a part of the original model. All possible sub-modules caused by model pruning are highly correlated because of the same origin.

To demonstrate the above analysis, we use DLLP and the most typical magnitude-based pruning methods to slim VGG-11 and count their parameter distributions. The figures which statistically visualize the parameter distributions of the original referenced model, the pruned model of DLLP, and the pruned models of magnitude-based SOTA including typical l_1 and l_2 regularization can be found in Appendix. Specifically, the distribution of the reference model has been proved to roughly obey the Gaussian distribution [24], which is consistent with our experiments. The results also show that typical magnitude-based pruning explicitly destroys the trained model distribution, even with sparsity regularization. Their pruned distributions are bimodal distributions and have to rely on the process of fine-tuning to return to the original distribution family. Finally, for the pruned model from DLLP, as expected, the pruned distribution still obeys a smooth Gaussian distribution, which not only saves the extra fine-tuning effort but also minimizes the distribution loss. Another strong piece of evidence comes from Figure 1. The 11-regular sparsely trained model roughly follows the Laplace distribution, which is consistent with its prior. And as expected, the model after DLLP sparse training obeys the spike-and-slab distribution, which helps achieve the proposed distribution-lossless pruning.

4.2.2 Pruned Model Reliability

Model pruning reduces the fit of the model parameters to the data and thus may lead to higher model uncertainty. Therefore, it is critical to analyze the task uncertainty of pruned models that will be deployed in edge environments. To the best of our knowledge, we are the first work that can simultaneously account for model uncertainty while model pruning.

In this subsection we examine two types of uncertainty that DLLP can cope with: Aleatoric uncertainty refers to the noise inherent in the observation sample/training

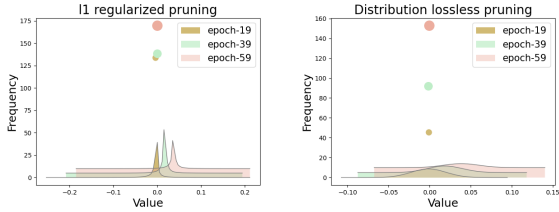


Figure 1: The comparison of layer-wise model distributions between l1-regularized pruning and DLLP. The models are sparsely trained before actual pruning. The vertical axis is the result of the bin’s raw count divided by the total number of counts and the bin width. To magnify the distribution difference, the bin nearest to zero is extracted and reflected in the colored circle. The larger the circle, the larger the count. Note that since DLLP has a very high spike distribution at zero, so the value of the corresponding circle has been subtracted by 225 for better presentation.

dataset, and epistemic uncertainty captures the model errors from the training [16].

Aleatoric Uncertainty. Define a function that maps from data quality to model aleatoric uncertainty. More specifically, the prediction results could be unreliable for samples with large noise, and the function value should be large. Conversely, for data with better quality (such as clear or prominent foreground samples), the model is more confident in its prediction results, and the value of prediction uncertainty should be smaller.

In order to demonstrate the above analysis, we conduct experiments with respect to the aleatoric uncertainty of VGG-11 predicting on processed Cifar-10 datasets. We apply Gaussian blur matrices with the radius of 1, 2, 3, and 5 pixels to the Cifar-10 dataset to reduce the high-frequency components of the image and add data noise with different levels. As analyzed in Section 3.1.1, we model the aleatoric uncertainty as the prediction variance in the likelihood function of the pruned models. The results are shown in Figure 2a.

Among them, sharpen is the data processed by Laplace sharpening, which is used to represent high-quality samples; gau-1, gau-2, gau-3, and gau-5 are Gaussian blurred data with radii of 1, 2, 3, and 5, respectively, used to represent different degrees of low-quality samples. As ex-

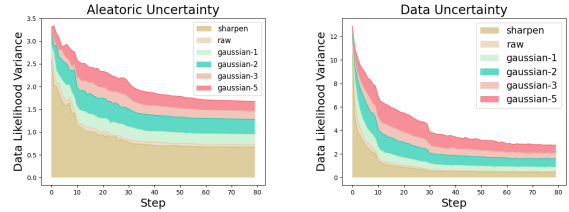


Figure 2: Model uncertainty reported by DLLP under five different data situations.

pected, as the quality of the data decreases, the arbitrary uncertainty of the predictions of the pruned model rises.

Epistemic Uncertainty Epistemic Uncertainty gives a measure of the extent to which the pruned sub-module is the causal model for the seen data domain. It comes from insufficient model training or insufficient observation samples. Define a function that maps from data quality to model epistemic uncertainty. Since the insufficient model training could be easily solved, the problem of insufficient observation would be our focus. To be specific, model predictions should be less reliable if there is not sufficient full data in the training domain, and the function value should be large. Conversely, if there are sufficient observations in the training domain during pruning, the retained sub-model will be more confident in its predictive ability, and the uncertainty function will be lower.

To demonstrate the above analysis, we test the epistemic uncertainty of pruned models on VGG-11 and Cifar-10 dataset. We randomly sample 20%, 40%, 60%, and 80% of the training set and check the prediction variance reported by the likelihood function. The results are shown in Figure 2b. As expected, the model epistemic uncertainty given by DLLP increases with decreasing observational data.

In summary, DLLP builds the model posterior distribution from a Bayesian perspective and sets the agnostic normalization parameters as learnable parameters. Therefore, DLLP can provide uncertainty measures for the current pruned sub-structures, and make this lightweight model more reliable.

Table 1: Performance comparison of pruning performance on ResNet-56 and Cifar-10.

Method	Original	Pruned	
	Acc. (%)	↓FLOPs	↓Acc. (%)
L1-norm [17]	93.42	34%	0.5
AMC [11]	92.80	50%	0.9
DCP [42]	93.80	50%	0.31
NS [23]	93.80	48%	0.53
SFP [10]	93.59	51%	0.24
CCP [2]	93.50	47%	0.04
FPGM [12]	93.59	53%	0.1
Deepfloyer [38]	93.80	48%	0.26
DLLP	92.80	55%	0.04

Table 2: Performance comparison of pruning performance on VGG-16 and Cifar-10.

Method	Original	Pruned	
	Acc. (%)	↓FLOPs	↓Acc. (%)
LIWS [36]	93.45	70.6%	0.8
ThiNet [25]	93.36	50%	0.14
CP [13]	93.18	50%	0.32
RNP [19]	92.15	50%	0.85
FBS [7]	93.03	50%	0.47
DLLP	92.80	74.65%	1.24

4.3 Comparison with SOTA

In this section, we compare the proposed DLLP with various SOTA methods including l_1 regularized pruning [17, 23], mixed l_1 and l_2 regularized pruning [38], polarization regularized pruning [41], reinforcement learning based pruning [11], etc. The performance comparison between different pruning methods is in terms of the model accuracy and FLOPs reduction.

The experiment results on Cifar-10 dataset with ResNet-56 and VGG-16 have been shown in Table 1 and Table 2, respectively. It can be seen that DLLP achieves the best performance on all structures including residual style and plain style. Specifically, as shown in Table. 1, DLLP achieves the smallest accuracy drop (0.04%) and

Table 3: Performance comparison of pruning performance on ResNet-50 and ImageNet.

Method	Original	Pruned	
	Acc. (%)	↓FLOPs	↓Acc. (%)
NS [23]	76.15	53%	1.27
SSS [15]	76.12	43%	4.30
DCP [42]	76.01	56%	1.06
CCP [2]	76.15	54%	0.94
SFP [10]	76.15	62.14%	14.01
DLLP	76.15	65.95%	6.13

the highest FLOPs reduction (55%) on ResNet-56 network, and the corresponding values are 1.24%, 74.65% for VGG-16 BN, which far exceeds the model compression ratio of existing SOTA.

The experiment results on ImageNet with ResNet-50 have been shown in Table 3. It can be seen that on a larger and more complicated dataset, DLLP still achieves the most significant FLOPs reduction (65.95%) with an accuracy drop close to SOTA’s. In summary, extensive experiments on Cifar-10 and ImageNet datasets have demonstrated that DLLP achieves state-of-the-art pruning performance.

5 Conclusion

In this paper, we analyze model pruning in principled Bayesian treatment and propose a novel distribution-lossless pruning method (DLLP). DLLP models the reference model as a spike-and-slab distribution to achieve distribution-lossless structure removal. What’s more, DLLP uses Stein Variational Inference to force the pruned distribution to gradually approach the true prior in an efficient gradient descent manner. Even better, DLLP can quantitatively provide a measure of the prediction uncertainty for the current pruning model. Extensive experiments have shown that compared to pruning SOTA, DLLP achieves a higher pruning rate along with satisfying accuracy.

References

- [1] Jincheng Bai, Qifan Song, and Guang Cheng. Efficient variational inference for sparse deep learning with theoretical guarantee. *Advances in Neural Information Processing Systems*, 33:466–476, 2020. [6](#)
- [2] Yanming Chen, Xiang Wen, Yiwen Zhang, and Weisong Shi. Ccprune: Collaborative channel pruning for learning compact convolutional networks. *Neurocomputing*, 451:35–45, 2021. [10](#)
- [3] Jifeng Dai, Kaiming He, and Jian Sun. Instance-aware semantic segmentation via multi-task network cascades. In *Proceedings of the IEEE conference on computer vision and pattern recognition*, pages 3150–3158, 2016. [1](#)
- [4] Pau de Jorge, Amartya Sanyal, Harkirat S. Behl, Philip H. S. Torr, Grégory Rogez, and Puneet K. Dokania. Progressive skeletonization: Trimming more fat from a network at initialization. In *9th International Conference on Learning Representations, ICLR 2021, Virtual Event, Austria, May 3-7, 2021*. OpenReview.net, 2021. [2](#)
- [5] Xuanyi Dong, Junshi Huang, Yi Yang, and Shuicheng Yan. More is less: A more complicated network with less inference complexity. In *Proceedings of the IEEE Conference on Computer Vision and Pattern Recognition*, pages 5840–5848, 2017. [3](#)
- [6] Xitong Gao, Yiren Zhao, Łukasz Dudziak, Robert Mullins, and Cheng-zhong Xu. Dynamic channel pruning: Feature boosting and suppression. *arXiv preprint arXiv:1810.05331*, 2018. [3](#)
- [7] Xitong Gao, Yiren Zhao, Lukasz Dudziak, Robert D. Mullins, and Cheng-Zhong Xu. Dynamic channel pruning: Feature boosting and suppression. In *7th International Conference on Learning Representations, ICLR 2019, New Orleans, LA, USA, May 6-9, 2019*. OpenReview.net, 2019. [10](#)
- [8] Song Han, Huizi Mao, and William J Dally. Deep compression: Compressing deep neural networks with pruning, trained quantization and huffman coding. *arXiv preprint arXiv:1510.00149*, 2015. [4](#)
- [9] Kaiming He, Xiangyu Zhang, Shaoqing Ren, and Jian Sun. Deep residual learning for image recognition. In *Proceedings of the IEEE conference on computer vision and pattern recognition*, pages 770–778, 2016. [1](#)
- [10] Yang He, Guoliang Kang, Xuanyi Dong, Yanwei Fu, and Yi Yang. Soft filter pruning for accelerating deep convolutional neural networks. In *Proceedings of the Twenty-Seventh International Joint Conference on Artificial Intelligence, IJCAI 2018, July 13-19, 2018, Stockholm, Sweden*, pages 2234–2240. ijcai.org, 2018. [10](#)
- [11] Yihui He, Ji Lin, Zhijian Liu, Hanrui Wang, Li-Jia Li, and Song Han. Amc: Automl for model compression and acceleration on mobile devices. In *Proceedings of the European conference on computer vision (ECCV)*, pages 784–800, 2018. [10](#)
- [12] Yang He, Ping Liu, Ziwei Wang, Zhilan Hu, and Yi Yang. Filter pruning via geometric median for deep convolutional neural networks acceleration. In *IEEE Conference on Computer Vision and Pattern Recognition, CVPR 2019, Long Beach, CA, USA, June 16-20, 2019*, pages 4340–4349. Computer Vision Foundation / IEEE, 2019. [10](#)
- [13] Yihui He, Xiangyu Zhang, and Jian Sun. Channel pruning for accelerating very deep neural networks. In *Proceedings of the IEEE international conference on computer vision*, pages 1389–1397, 2017. [10](#)
- [14] Weizhe Hua, Yuan Zhou, Christopher M De Sa, Zhiru Zhang, and G Edward Suh. Channel gating neural networks. *Advances in Neural Information Processing Systems*, 32, 2019. [3](#)
- [15] Zehao Huang and Naiyan Wang. Data-driven sparse structure selection for deep neural networks. In *ECCV (16)*, volume 11220 of *Lecture Notes in Computer Science*, pages 317–334. Springer, 2018. [10](#)
- [16] Alex Kendall and Yarin Gal. What uncertainties do we need in bayesian deep learning for computer vision? *Advances in neural information processing systems*, 30, 2017. [7, 9](#)
- [17] Hao Li, Asim Kadav, Igor Durdanovic, Hanan Samet, and Hans Peter Graf. Pruning filters for efficient convnets. In *5th International Conference on Learning Representations, ICLR 2017, Toulon, France, April 24-26, 2017, Conference Track Proceedings*. OpenReview.net, 2017. [10](#)
- [18] Lucas Liebenwein, Cenk Baykal, Harry Lang, Dan Feldman, and Daniela Rus. Provable filter pruning for efficient neural networks. In *International Conference on Learning Representations*, 2019. [3](#)
- [19] Ji Lin, Yongming Rao, Jiwen Lu, and Jie Zhou. Runtime neural pruning. In *Proceedings of the 31st International Conference on Neural Information Processing Systems*, pages 2178–2188, 2017. [10](#)
- [20] Qiang Liu, Jason Lee, and Michael Jordan. A kernelized stein discrepancy for goodness-of-fit tests. In *International conference on machine learning*, pages 276–284. PMLR, 2016. [3](#)
- [21] Qiang Liu and Dilin Wang. Stein variational gradient descent: A general purpose bayesian inference algorithm. *Advances in neural information processing systems*, 29, 2016. [2, 3, 6](#)

- [22] Zhuang Liu, Jianguo Li, Zhiqiang Shen, Gao Huang, Shoumeng Yan, and Changshui Zhang. Learning efficient convolutional networks through network slimming. In *Proceedings of the IEEE international conference on computer vision*, pages 2736–2744, 2017. 3
- [23] Zhuang Liu, Jianguo Li, Zhiqiang Shen, Gao Huang, Shoumeng Yan, and Changshui Zhang. Learning efficient convolutional networks through network slimming. In *Proceedings of the IEEE international conference on computer vision*, pages 2736–2744, 2017. 10
- [24] Zhuang Liu, Mingjie Sun, Tinghui Zhou, Gao Huang, and Trevor Darrell. Rethinking the value of network pruning. In *7th International Conference on Learning Representations, ICLR 2019, New Orleans, LA, USA, May 6-9, 2019*. OpenReview.net, 2019. 4, 8
- [25] Jian-Hao Luo, Jianxin Wu, and Weiyao Lin. Thinet: A filter level pruning method for deep neural network compression. In *Proceedings of the IEEE international conference on computer vision*, pages 5058–5066, 2017. 10
- [26] Dmitry Molchanov, Arsenii Ashukha, and Dmitry Vetrov. Variational dropout sparsifies deep neural networks. In *International Conference on Machine Learning*, pages 2498–2507. PMLR, 2017. 6
- [27] Pavlo Molchanov, Arun Mallya, Stephen Tyree, Iuri Frosio, and Jan Kautz. Importance estimation for neural network pruning. In *Proceedings of the IEEE/CVF Conference on Computer Vision and Pattern Recognition*, pages 11264–11272, 2019. 3
- [28] James Pickands III. Statistical inference using extreme order statistics. *the Annals of Statistics*, pages 119–131, 1975. 5
- [29] Yongming Rao, Jiwen Lu, Ji Lin, and Jie Zhou. Runtime network routing for efficient image classification. *IEEE transactions on pattern analysis and machine intelligence*, 41(10):2291–2304, 2018. 3
- [30] Shaoqing Ren, Kaiming He, Ross Girshick, and Jian Sun. Faster r-cnn: Towards real-time object detection with region proposal networks. *Advances in neural information processing systems*, 28, 2015. 1
- [31] Hidenori Tanaka, Daniel Kunin, Daniel L Yamins, and Surya Ganguli. Pruning neural networks without any data by iteratively conserving synaptic flow. *Advances in Neural Information Processing Systems*, 33:6377–6389, 2020. 2
- [32] Yehui Tang, Yunhe Wang, Yixing Xu, Yiping Deng, Chao Xu, Dacheng Tao, and Chang Xu. Manifold regularized dynamic network pruning. In *Proceedings of the IEEE/CVF Conference on Computer Vision and Pattern Recognition*, pages 5018–5028, 2021. 3
- [33] Yehui Tang, Yunhe Wang, Yixing Xu, Yiping Deng, Chao Xu, Dacheng Tao, and Chang Xu. Manifold regularized dynamic network pruning. In *Proceedings of the IEEE/CVF Conference on Computer Vision and Pattern Recognition*, pages 5018–5028, 2021. 3
- [34] Yehui Tang, Yunhe Wang, Yixing Xu, Dacheng Tao, Chun-jing Xu, Chao Xu, and Chang Xu. Scop: Scientific control for reliable neural network pruning. *Advances in Neural Information Processing Systems*, 33:10936–10947, 2020. 3
- [35] Chaoqi Wang, Guodong Zhang, and Roger Baker Grosse. Picking winning tickets before training by preserving gradient flow. *CoRR*, abs/2002.07376, 2020. 2
- [36] Yulong Wang, Xiaolu Zhang, Xiaolin Hu, Bo Zhang, and Hang Su. Dynamic network pruning with interpretable layerwise channel selection. In *Proceedings of the AAAI Conference on Artificial Intelligence*, volume 34, pages 6299–6306, 2020. 10
- [37] Wei Wen, Chunpeng Wu, Yandan Wang, Yiran Chen, and Hai Li. Learning structured sparsity in deep neural networks. *Advances in neural information processing systems*, 29, 2016. 3
- [38] Huanrui Yang, Wei Wen, and Hai Li. Deepphoyer: Learning sparser neural network with differentiable scale-invariant sparsity measures. In *8th International Conference on Learning Representations, ICLR 2020, Addis Ababa, Ethiopia, April 26-30, 2020*. OpenReview.net, 2020. 10
- [39] Michael Zhu and Suyog Gupta. To prune, or not to prune: Exploring the efficacy of pruning for model compression. In *6th International Conference on Learning Representations, ICLR 2018, Vancouver, BC, Canada, April 30 - May 3, 2018, Workshop Track Proceedings*. OpenReview.net, 2018. 3
- [40] Tao Zhuang, Zhixuan Zhang, Yuheng Huang, Xiaoyi Zeng, Kai Shuang, and Xiang Li. Neuron-level structured pruning using polarization regularizer. In Hugo Larochelle, Marc’Aurelio Ranzato, Raia Hadsell, Maria-Florina Balcan, and Hsuan-Tien Lin, editors, *Advances in Neural Information Processing Systems 33: Annual Conference on Neural Information Processing Systems 2020, NeurIPS 2020, December 6-12, 2020, virtual*, 2020. 4
- [41] Tao Zhuang, Zhixuan Zhang, Yuheng Huang, Xiaoyi Zeng, Kai Shuang, and Xiang Li. Neuron-level structured pruning using polarization regularizer. In H. Larochelle, M. Ranzato, R. Hadsell, M.F. Balcan, and H. Lin, editors, *Advances in Neural Information Processing Systems*, volume 33, pages 9865–9877. Curran Associates, Inc., 2020. 10

- [42] Zhuangwei Zhuang, Mingkui Tan, Bohan Zhuang, Jing Liu, Yong Guo, Qingyao Wu, Junzhou Huang, and Jinhui Zhu. Discrimination-aware channel pruning for deep neural networks. *Advances in neural information processing systems*, 31, 2018. 10